Correlation of the Kinetics of Finger Domain Mutants in RB69 DNA Polymerase with Its Structure†

Guangwei Yang, Matthew Franklin, Jing Li, T.-C. Lin, and William Konigsberg*

Department of Molecular Biophysics and Biochemistry, Yale University, 333 Cedar Street, New Haven, Connecticut 06520

Received October 30, 2001; Revised Manuscript Received December 19, 2001

ABSTRACT: We have estimated pre-steady-state kinetic parameters for the addition of a single nucleotide residue by a set of RB69 DNA polymerase mutants in which four highly conserved residues in the fingers domain have been replaced by Ala. The relationship between the kinetic constants exhibited by the mutants and the structure of the ternary complex [Franklin, M., Wang, J., and Steitz T. (2001) *Cell 105*, 657−667] was consistent with the following sets of interactions between the conserved residues and oxygen atoms in the triphosphate portion of the incoming dNTP: (i) the ϵ-amino group of K560 contacts oxygen atoms of the α- and γ-phosphates, (ii) the amide side chain of Asn 564 forms a hydrogen bond via a water molecule with the nonbridging oxygen of the β-phosphate, and (iii) the ϵ-amino and δ-guanidino groups of K486 and R482, respectively, contact the nonbridging oxygens of the γ-phosphate. We have also determined the pre-steady-state kinetic parameters for the addition of both dCTP and dCDP onto a 13/20mer primer/template with an exo$^-$ derivative of RB69 DNA polymerase and have shown that the deoxynucleoside diphosphate can be incorporated, in contrast to the behavior of the Klenow fragment which cannot use dCDP as a substrate. We have shown that, with RB69 DNA polymerase, in contrast to the Klenow fragment, there is no inhibition of the primer-extension reaction by incoming NTPs having either noncomplementary bases or ribo- instead of a deoxyribose moieties. This implies that the mode of recognition of incoming dNTPs and triggering of the conformational change, which is thought to occur prior to the chemical step, differs between these two enzymes.

DNA polymerases constitute the central catalytic component of the replisome, a multiprotein complex responsible for faithful duplication of genetic material. Even though DNA polymerases have diverse sequences, they share two common motifs, A and C, which contain two absolutely conserved catalytic metal-binding aspartate residues essential for catalysis (*1*, *2*). There are other clusters of sequence similarities (regions I−V) found only in some DNA polymerases which serve as hallmarks, allowing the polymerases to be grouped into separate families (*3*).

T4 and RB69 DNA polymerases have 62% sequence identity, possess pol[1] and exo activities, and belong to the pol α family (*4*). Both of these phage-encoded enzymes have received considerable attention: T4 DNA polymerase because it has been used for extensive mutagenesis and kinetic studies (*5*−*13*) and RB69 DNA polymerase (RB69 gp43) because of its ability to crystallize, facilitating determination of its structure in several forms. These include the apoenzyme (*14*); a binary complex with a frayed primer/template (PT) in the "exo" or editing mode, a conformation poised for excision of the 3′-terminal nucleotide residue (*15*); and a ternary complex in the "pol" mode with a dideoxy-terminated PT and a dNTP complementary to the first unpaired base in the template strand (*16*).

Comparison of the three different RB69 gp43 structures has provided an opportunity to assess the extent of the conformational changes that occur when the enzyme goes from the unliganded state to a binary complex in the exo mode and to a ternary complex capable of catalyzing the nucleotidyl transfer reaction. Among the motifs shared by polymerases in all the families, motif B (KXXNFGXXYG in the pol I family and KXXXNSXYG in the pol α family) (*17*) interacts with nucleotide residues of a nascent base pair and binds to the triphosphate moiety of incoming dNTPs (*16*, *18*, *19*). Motif B is in the fingers domain which undergoes the largest conformational change when the polymerase goes from an unliganded state to a ternary complex poised for nucleotide addition (Figure 1A) (*16*). When this occurs, the conserved residues in motif B move closer to the active site and may actually participate in the reaction mechanism. Structures of four other pol α family DNA polymerases have recently been reported (*20*−*23*) that have many features in common with RB69 gp43. Whether the kinetic results obtained with RB69 gp43 are applicable to other pol α family members and perhaps to replicative polymerases such as HIV RT that belong to other families remains to be determined.

† This work was supported by U.S. Public Health Service Grants GM63276-01 to W.H.K. and GM57510 to Thomas A. Steitz.

* To whom correspondence and reprint requests should be addressed. Tel: 203-785-4599. Fax: 203-785-7979. E-mail: william.konigsberg@yale.edu.

[1] Abbreviations: dCTP, deoxycytidine triphosphate; dCDP, deoxycytidine diphosphate; PP_i, pyrophosphate; RB69 gp43, RB69 DNA polymerase; KF, Klenow fragment; pol, polymerase, exo, 3′−5′ exonuclease; PT, primer/template; k_{ss}, steady-state rate constant; k_{pol}, maximum rate of nucleotide incorporation; k_{ob}, observed first-order rate constant for dNTP incorporation; K_d, dissociation constant for dNTP binding.

10.1021/bi0119924 CCC: $22.00
Published on Web 01/31/2002

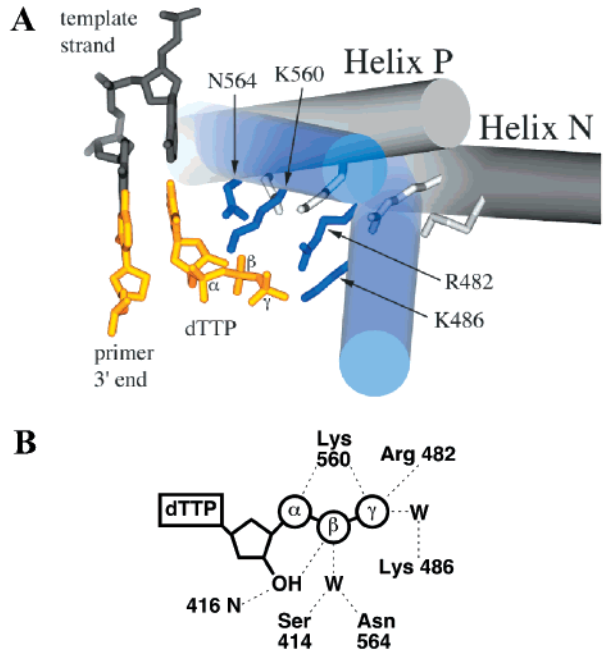

FIGURE 1: (A) Movement of the fingers domain. The structures of RB69 pol in its apo form (PDB code 1WAJ) (*14*) and in its ternary complex form (PDB code 1IG9) (*16*) were superimposed on the palm domain, with a Cα RMSD of 0.89 Å over 264 residues. Fingers helices N and P of the superimposed structures are shown as cylinders (helix P is truncated at residue 551 for clarity), with the side chains of residues 482, 486, 560, and 564 shown in stick form. The residues and helices from the apo RB69 gp43 structure are colored gray, while those from the ternary complex structure are in blue. Also shown in stick form are two bases of the template DNA from the ternary complex (in dark gray), the 3′-terminal base of the primer DNA (in gold), and the bound dTTP (in gold) with its α-, *β*-, and *γ*-phosphates labeled. (B) Schematic diagram of interactions between the polymerase and the triphosphate moiety of an incoming dNTP. The bound dTTP of the RB69 gp43 ternary complex (PDB code 1IG9) (*16*) is shown with the base represented by a rectangle, the ribose ring represented by a pentagon with a protruding 3′-OH, and the α-, *β*-, and *γ*-phosphates represented by circles. Hydrogen bonds are shown as dashed lines. W indicates a water molecule mediating a hydrogen bond between protein and dTTP; 416 N indicates the main-chain amide of Tyr 416. All other hydrogen bonds involve side chains of the residues indicated.

The general mechanism for primer extension catalyzed by DNA polymerases involves a number of steps which include PT binding followed by formation of a ternary complex with an incoming dNTP. It has been proposed that this last step induces a conformational change in the polymerase if the incoming dNTP is complementary to the corresponding template base (*24*). It has also been suggested that this conformational change leads to a "closed" ternary complex capable of catalyzing the chemical step that requires the presence of two divalent metal ions (*2*, *25*). After formation of the phosphodiester bond, the newly extended PT translocates, with dissociation of pyrophosphate, allowing addition of the next nucleotide residue. All DNA polymerases including those in the pol I and pol α families utilize the same two metal ion mechanism but the kinetic parameters differ, which may have important biological implications (*24*).

Single site mutants in RB69 gp43 were constructed to examine the functional consequences of disrupting interactions of four of the conserved residues in the fingers domain with the oxygen atoms in the triphosphate moiety of an incoming dNTP. We previously reported changes in steady-state kinetic parameters exhibited by a set of four of these mutants (*26*), and the results were consistent with the crystal structure of the RB69 gp43 ternary complex. Comparison of the structures of RB69 gp43 in the apo form and in the ternary complex shows that the fingers domain undergoes a conformational change with a 60° rotation toward the active site of the polymerase, and as a consequence, two residues in helix P (K560 and N564) and two residues in helix N (R482 and K486) in the fingers domain are shifted to positions that allow them to interact with the triphosphate moiety of the incoming dNTP (*16*). Whether these events are concerted or sequential is not known. To address this issue, we have performed pre-steady-state kinetic experiments using the parental (exo$^-$) enzyme and four of the finger domain mutants. We also show that dCDP acts both as a substrate and as an inhibitor of primer extension with RB69 gp43 but not with the Klenow Fragment (KF). Finally, we discuss the mechanistic and biological implications of the differences in behavior between RB69 gp43 and KF with respect to inhibition of primer extension by mismatched dNTPs and by rNTPs.

EXPERIMENTAL PROCEDURES

Materials

T4 polynucleotide kinase was obtained from New England Biolabs; dCDP, dCMP, and pyrophosphate were from Sigma; [γ-^{32}P]ATP was from Perkin-Elmer Life Sciences, Inc.; dNTPs and dCTPαS were from Amersham Pharmacia Biotech Corp.; electrophoresis reagents were from American Bioanalytical Corp. dΦTP (abasic nucleoside triphosphate) was kindly provided by Dr. Eric Kool (Stanford University). Oligonucleotides were synthesized by the W. M. Keck Foundation Biotechnology Resource Laboratory (Yale University). All other chemicals used were of analytical grade. Mutant derivatives of RB69 gp43 were constructed and purified as described previously (*26*). All of the RB69 gp43 derivatives used in this study carry the D222A/D327A double mutation that eliminates the 3′−5′ exonuclease activity. The DNA duplex (13/20GT) used as primer/template had the following sequence: 13mer, 5′-CCGACCAGCCTTG-3′; 20mer, 3′-GGCTGGTCGGAACGTTTTTT-5′. The 13mer was 5′-labeled with γ-^{32}P by standard procedures, annealed with the complementary 20mer, and used as substrate for primer extension assays.

Methods

Pre-Steady-State Burst and Single-Turnover Experiments. Pre-steady-state rapid chemical quench experiments were performed with the KinTek quench-flow apparatus (model RQF-3, KinTek Corp., University Park, PA). For slower reactions, requiring sampling at time intervals of >20 s, aliquots were quenched manually. Unless noted otherwise, all components of the reactions are reported as final concentrations after mixing.

Burst assays were carried out under the conditions in which the PT concentration was three times greater than that of the enzyme. The reaction was carried out at 25 °C by mixing equal volumes of 66 mM Tris-HCl, pH 7.5, containing the preincubated complex of 2 μM 5′-^{32}P-labeled PT and 600

nM RB69 gp43 parental exo$^-$ enzyme (or its mutants) with 66 mM Tris-HCl, pH 7.5, containing 20 mM $MgSO_4$ and 2 mM dCTP to give final concentrations of 1 μM PT, 300 nM enzyme, and 1 mM dCTP. The polymerization reaction was quenched with 0.5 mM EDTA at defined time intervals. Products were analyzed by gel electrophoresis (20% polyacrylamide/50% urea) and quantified by gel scanning using a phosphorimager (Molecular Dynamics). Single-turnover assays were performed in a manner similar to that described above except that the enzyme (2 μM) was used in excess of the PT (300 nM), and concentrations of dCTP (or other dCTP-related compounds) were varied to determine K_d and k_{pol} values.

Pre-Steady-State Inhibition Assays. Commercial dCDP was purified by HiTrap Q column chromatography (Pharmacia) to remove the contaminating dCTP and dCMP. A linear gradient of 20−500 mM ammonium bicarbonate, pH 8.5, was applied for elution with a flow rate of 2 mL/min. dCMP eluted first, followed by dCDP and dCTP. Ammonium bicarbonate in the purified dCDP was removed by freeze-drying.

Inhibition assays were performed in a manner similar to that of the single-turnover assays except that various concentrations (0.1−2 mM) of dCTP-related compounds were included in the reaction mixture with 10 μM dCTP (the correct incoming nucleotide).

Elemental Effects on the Polymerization Reaction. Assays to estimate the elemental effect were carried out under single-turnover conditions described above except that dCTPαS (S_p) and dCTPαS ($S_p + R_p$) were used instead of dCTP.

Pyrophosphorolysis. The primer/template 13/20GT was used in the determination of the kinetic constants K_d and k_{PP_i} for pyrophosphorolysis, the reverse reaction of primer extension. Assays were carried out under single-turnover conditions with 300 nM PT, 2 μM enzyme, and varying concentrations of PP_i.

Data Analysis. Data from burst assays were fit to a burst equation:

$$[\text{product}] = A(1 - e^{-k_{ob}t}) + k_{ss}t$$

where A represents the amplitude of the burst experiment which correlates with the concentration of enzyme in active form, k_{ob} is the observed first-order rate constant for dNTP incorporation, and k_{ss} is the observed steady-state rate constant.

Data from single-turnover experiments were fit to a single-exponential equation. The K_d, the dissociation constant of nucleotide binding to the RB69 gp43−13/20mer (E−PT) complex, was calculated by fitting the data to the equation:

$$k = k_{pol}[S]/(K_d + [S])$$

where k_{pol} is the maximum rate for dNTP incorporation, [S] is the concentration of incoming nucleotide, and K_d is the equilibrium dissociation constant for the interaction of incoming dNTP with the E−PT complex.

RESULTS

Burst Assays. Burst experiments were performed primarily to determine the active site concentration of the enzyme as well as to observe the initial rate of dNTP incorporation and, second, to observe the steady-state rate (k_{ss}) for the nucleotidyl transfer reaction under saturating concentrations of dCTP. For pre-steady-state experiments, concentrations of both the PT and the enzyme exceeded the K_d of the E−PT complex which was reported to be 70 nM (*5*) for T4 DNA polymerase bound to a 13/20mer PT. We have assumed that RB69 gp43 has a similar value. The time course for incorporation of dCTP into the 13/20mer by the parental enzyme, as well as by the K486A and N564A mutants, is shown in Figure 2. For the parental enzyme, the rate of product formation (13C/20mer) is biphasic. The best fit of the data gave an amplitude, A, of 225 nM, indicating that

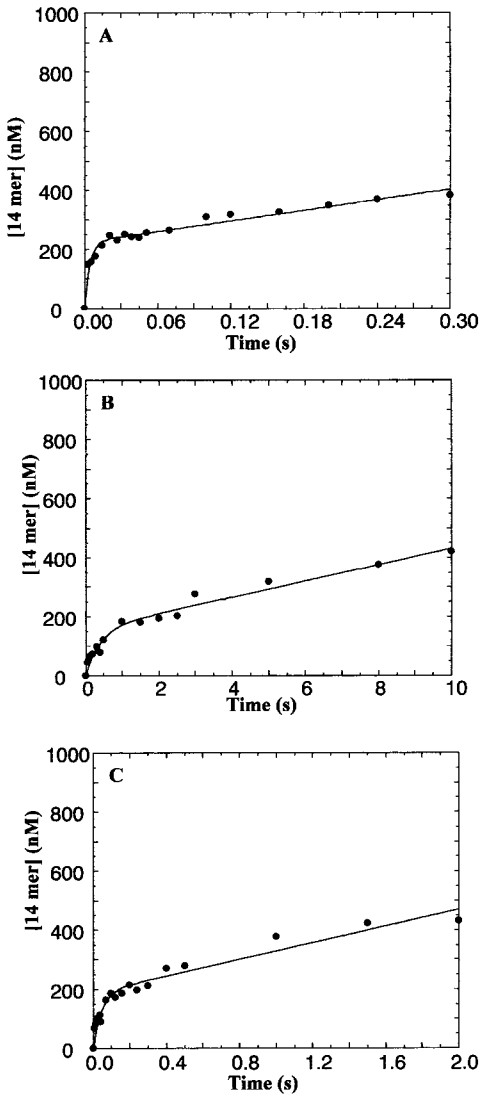

FIGURE 2: Burst assays for parental RB69 gp43, K486A, and N564A. A preincubated 13/20mer (2 μM) with RB69 gp43 or its mutants (600 nM) was mixed with an equal volume of 2 mM dCTP in 20 mM Mg^{2+} containing Tris-HCl, pH 7.5, buffer to start the reaction, giving final concentrations of 1 μM 13/20mer, 300 nM enzyme, 1 mM dCTP, and 10 mM Mg^{2+}. The reactions were quenched at the indicated times and analyzed by gel electrophoresis. The solid lines represent the fit to the burst equation as described in Experimental Procedures. (A) Burst assay for the parental RB69 gp43 gave an amplitude, A, of 225 nM, a burst rate, k_{ob}, of 232 ± 35 s^{-1}, and a steady-state rate, k_{ss}, of 2.7 ± 0.2 s^{-1}. (B) Burst assay for K486A gave an amplitude, A, of 160 nM, a burst rate, k_{ob}, of 2.6 ± 0.6 s^{-1}, and a steady-state rate, k_{ss}, of 0.17 ± 0.02 s^{-1}. (C) Burst assay for N564A gave an amplitude, A, of 190 nM, a burst rate, k_{ob}, of 22 ± 5 s^{-1}, and a steady-state rate, k_{ss}, of 0.75 ± 0.08 s^{-1}.

Table 1: Burst Assays for the Parental Enzyme (exo$^-$ RB69 gp43) and for Mutants in the Fingers Domain

enzyme	amplitude (nM)	k_{ob} (s^{-1})	k_{ss} (s^{-1})
parental	225	232 ± 35	2.7 ± 0.2
K486A	160	2.6 ± 0.6	0.17 ± 0.02
N564A	190	22 ± 5	0.75 ± 0.08
R482A	nb[a]	nb	nb
K560A	nb	nb	nb

[a] nb: no burst was observed.

Table 2: Elemental Effect of the Parental Enzyme and the Finger Domain Mutants

(A) Assay Using dCTPαS (S_p)[a]

	rate (s^{-1})		
enzyme	dCTP	dCTPαS(S_p)	elemental effect
parental	46	20	2
K486A	0.85	0.52	2

(B) Assay Using dCTPαS ($S_p + R_p$)[b]

	rate (s^{-1})		
enzyme	dCTP	dCTPαS ($S_p + R_p$)	elemental effect[c]
parental	170	42	2
R482A	0.07	0.03	1
K486A	2.7	0.9	2
K560A	0.3	0.04	4
N564A	17	2.0	4

[a] Conditions: 2 μM enzyme, 0.3 μM PT, and 10 μM dCTP or dCTPαS (S_p), pH 7.5, 25 °C. [b] Conditions: 2 μM enzyme, 0.3 μM PT, and 0.5 mM dCTP or 1 mM dCTPαS ($S_p + R_p$), pH 7.5, 25 °C. [c] Due to the difficulty in preparing enough dCTPαS (S_p) for these experiments, we used dCTPαS containing an equal amount of the R_p and S_p forms. The elemental effect using the $S_p + R_p$ mixture was estimated by dividing the $k_{dCTP}/k_{dCTP\alpha S}$ values by 2 because the R_p form is a competitive inhibitor. The justification for using this procedure is supported by the consistent values of the elemental effect for the parental enzyme and the K486A mutant as can been seen above in (A) and (B).

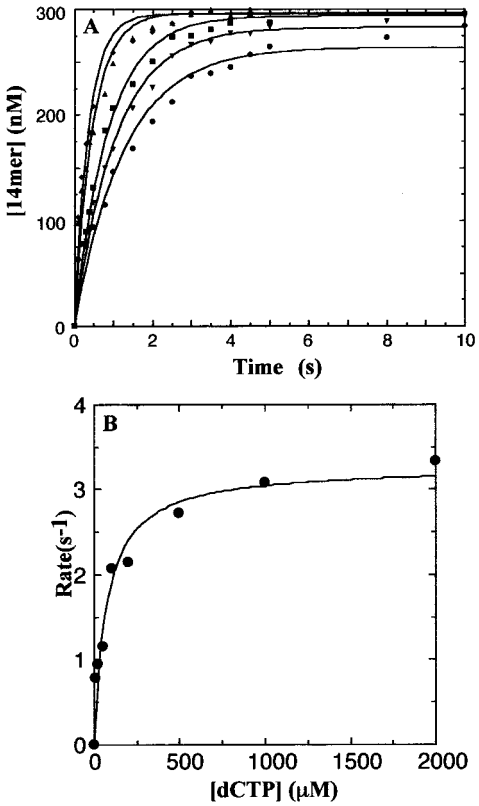

FIGURE 3: Single-turnover assays for determination of K_d and k_{pol} for K486A. (A) K486A (4 μM) and 13/20mer (600 nM) were preincubated and mixed with equal volumes of increasing concentrations of dCTP in 20 mM Mg^{2+} containing Tris-HCl buffer, pH 7.5, to start the reaction. The reactions were quenched at the indicated times and analyzed by gel electrophoresis. The dCTP concentrations were 10 μM (●), 25 μM (▼), 50 μM (■), 200 μM (▲), and 500 μM (◆). The solid lines represent the best fit of the data to a single exponential. (B) The pre-steady-state rates were plotted against the dCTP concentrations and fit to the equation for K_d/k_{pol} determination as described in Experimental Procedures to give a K_d of 71 μM and a k_{pol} of 3.3 s^{-1}.

only 75% of the PT is in a productively bound form. The pre-steady-state rate for the nucleotide addition (k_{ob}) and the steady-state rate (k_{ss}) (Table 1) are comparable to the data on T4 DNA polymerase (k_{pol} of 400 s^{-1}, k_{ss} of 2 s^{-1} at pH 8.8, 20 °C) reported by Capson et al. (*5*). The K486A and the N564A mutants also show bursts with biphasic kinetics (Table 1 and Figure 2). The fact that bursts were observed with the parental enzyme as well as with the K486A and N564A mutants indicates that the rate-limiting step occurs after chemistry. No burst was observed with the R482A and K560A mutants, suggesting that chemistry or steps before chemistry were rate-limiting with these enzymes.

Elemental Effects on the Polymerization Reaction. Experiments to estimate the elemental effect were performed under single-turnover conditions to determine whether the chemical step was rate-limiting for polymerization. The parental enzyme and all of the four mutants in the fingers domain showed elemental effects between 1 and 4 (Table 2), values below what is considered to be indicative of a rate-limiting chemical step (*27*).

Rates for dCTP Incorporation Determined from Single-Turnover Assays. We determined the pre-steady-state K_d and k_{pol} values for the parental enzyme and the four finger domain mutants under single-turnover conditions by varying the concentration of incoming dCTP (Figure 3 and Table 3). An example of the data obtained for the determination of K_d and k_{pol} with the K486A mutant is shown in Figure 3. The parental enzyme had K_d and k_{pol} values for dCTP incorporation consistent with those reported by Capson et al. (*5*). Among the finger domain mutants, N564A exhibited a higher K_d and a lower k_{pol} relative to the parental enzyme. K486A had a K_d nearly identical to that of the parental enzyme; however, the k_{pol} was greatly reduced (Table 3). The other two mutants, R482A and K560A, had much higher K_d and lower k_{pol} values compared to the parental enzyme. The low k_{pol} values are consistent with our observation that there was no burst with either of these two mutants. Overall, the catalytic efficiencies (k_{pol}/K_d) for all four mutants were lower than for the parental enzyme.

Pre-Steady-State Kinetic Parameters for Incorporation of Various Potential Substrates by the Parental Enzyme. The pre-steady-state behavior of wild-type RB69 gp43 showed much higher K_d values (4−16 mM) as well as lower k_{pol} (less than 1 s^{-1}) values for the pseudosubstrates rCTP, ddCTP, and dGTP than for the correct substrate, dCTP (Table 4). A comparison of our results with those determined for KF shows that, in contrast to RB69 gp43, KF has only slightly higher K_d values for rCTP, ddCTP, and a mismatched dNTP but dramatically lower k_{pol}'s relative to a correctly matched dNTP, indicating that KF has similar binding

Table 3: Pre-Steady-State Kinetic Parameters for dCTP and dCDP Incorporation into the 13/20mer PT by the Parental Enzyme and Finger Domain Mutants[a]

	dCTP			dCDP		
enzyme	K_d (μM)	k_{pol} (s^{-1})	k_{pol}/K_d ($s^{-1}\cdot\mu M^{-1}$)	K_d (μM)	k_{pol} (s^{-1})	k_{pol}/K_d ($s^{-1}\cdot\mu M^{-1}$)
parental	69	200[b]	2.9	1.2×10^3	0.50	4.2×10^{-4}
R482A	1.1×10^3	0.21	1.9×10^{-4}	140	1.6×10^{-3}	1.1×10^{-5}
K486A	71	3.3	4.6×10^{-2}	5.8×10^3	0.18	3.1×10^{-5}
K560A	790	0.8	1.0×10^{-3}	1.8×10^3	1.4×10^{-3}	7.7×10^{-7}
N564A	250	23	9.2×10^{-2}	480	0.02	4.2×10^{-5}

[a] Single-turnover assays were carried out at 25 °C with 2 μM enzyme, 300 nM PT, and varying concentrations of dCTP (or dCDP) to determine K_d and k_{pol} values. [b] When the assays were carried out at pH 8.8, the k_{pol} was 400 s^{-1}, consistent with the value determined by Capson et al. (*4*).

Table 4: Comparison of Pre-Steady-State Kinetic Parameters for Utilization of Potential Substrates for RB69 gp43 and KF[a]

	RB69 gp43		KF	
	K_d (μM)	k_{pol} (s^{-1})	K_d (μM) (ref)	k_{pol} (s^{-1}) (ref)
potential substrate				
dCTP (correct sugar, correct base)	69	200	9.6 (*29*)	75 (*29*)
dGTP (wrong base, correct sugar)	$\sim 9 \times 10^3$	0.1	214 (*31*)	0.028 (*31*)
rCTP (correct base)	$\sim 1.6 \times 10^4$	0.74	21 (*29*)	0.047 (*29*)
ddCTP (wrong sugar)	$\sim 4 \times 10^3$	0.17	8.4 (*28*)	0.015 (*28*)
reaction product				
PP_i	$\sim 2.6 \times 10^4$	0.35	100 (*32*)	0.12 (*32*)

[a] Single-turnover assays were carried out at 25 °C with 2 μM enzyme, 300 nM PT, and varying concentrations of dCTP (or other dCTP-related compounds) to determine K_d and k_{pol} values.

affinity for correct and incorrectly matched substrates (Table 4) (*28*−*31*).

Pyrophosphorolysis Experiments with the Parental Enzyme. We measured the dissociation constant for pyrophosphate (PP_i) by examining the kinetics of the pyrophosphorolysis reaction with the parental (exo$^-$) form of RB69 gp43. The dependence of the rate of pyrophosphorolysis on the concentration of PP_i provided estimates of the K_d for PP_i (Table 4) which agreed with the results of Capson et al. (*5*). KF, however, had a K_d value of 100 μM for PP_i in the pyrophosphorolysis reaction, which is only 10-fold higher than the K_d for dCTP (Table 4) (*32*).

Inhibition of dCTP Incorporation by dCTP-Related Compounds. Competition experiments were performed to measure the effect of dCTP analogues on the rate of dCTP incorporation. It was expected that if an analogue had an affinity similar to that of dCTP, the rate of primer extension would decrease. Six dCTP analogues, dCDP, dCMP, rCTP, dTTP (having a noncomplementary base), dΦTP (without any base), and PP_i were tested as potential inhibitors. We estimated the rate of conversion of a 13/20mer into a 14/20mer using 10 μM dCTP with varying concentrations of analogues (up to 2 mM). We found that the rate of dCTP incorporation was reduced only by dCDP but not by any of the other compounds. dCDP inhibited dCTP incorporation with an estimated K_i of 0.5 mM (Figure 4). With KF, correct dTTP incorporation was inhibited by the noncomplementary dATP with a K_i of 20 μM, the same as the K_d for dTTP (*33*). No information on inhibition is available for the other deoxynucleoside derivatives with KF.

Pre-Steady-State Kinetic Parameters for dCDP Incorporation. We previously reported that several mutants in the fingers domain could utilize deoxynucleoside diphosphates for primer extension. We then determined steady-state kinetic parameters for dGDP incorporation (*26*), but no dGDP incorporation with the parental enzyme was observed at that time because of trace amounts of contaminating exonuclease in the parental RB69 gp43. We have succeeded in removing all of the exonuclease contamination so that we can now demonstrate dCDP incorporation by the parental enzyme (Figure 5A). However, using the same assays, we failed to detect dCDP incorporation by T7 DNA polymerase or KF (both in their exo$^-$ forms). We did observe a burst for dCDP incorporation by the parental RB69 gp43, with a k_{ob} of 0.26 $\pm$ 0.07 s^{-1} and a k_{ss} of 0.04 $\pm$ 0.01 s^{-1} (Figure 5B), indicating that the rate-limiting step occurs after chemistry. We then determined the pre-steady-state kinetic parameters for the parental RB69 gp43 and the four finger domain mutants under single-turnover conditions (Table 3). The parental enzyme and all of the mutants except R482A had higher K_d values for dCDP relative to dCTP. The k_{pol}'s for dCDP vs dCTP incorporation exhibited by the parental enzyme and each of the mutants were reduced by factors that varied from 18 for K486A to 1150 for N564A. It is of interest that the K486A mutant, which had the smallest

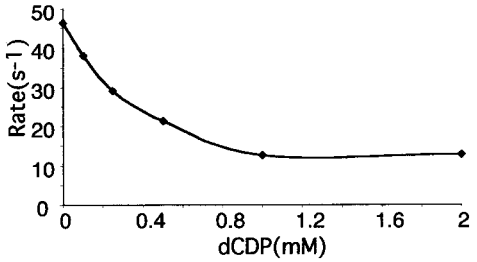

FIGURE 4: Inhibition of dCTP incorporation by dCDP. The rates of incorporation of dCTP (10 μM) into 13/20mer (300 nM) with 2 μM parental RB69 gp43 at 0, 0.1, 0.25, 0.5, 1, and 2 mM dCDP were shown. The plot of the rates vs dCDP concentration gave an estimated K_i of 0.5 mM. We could not observe increased inhibition even if the dCDP concentration was raised to 2 mM. Among the possible reasons for this are (i) traces of impurities in the dCDP (we could still detect about 0.05−0.08% dCTP in the dCDP, even after extensive purification) and (ii) dCDP can still be utilized for primer extension albeit with low efficiency by the parental enzyme.

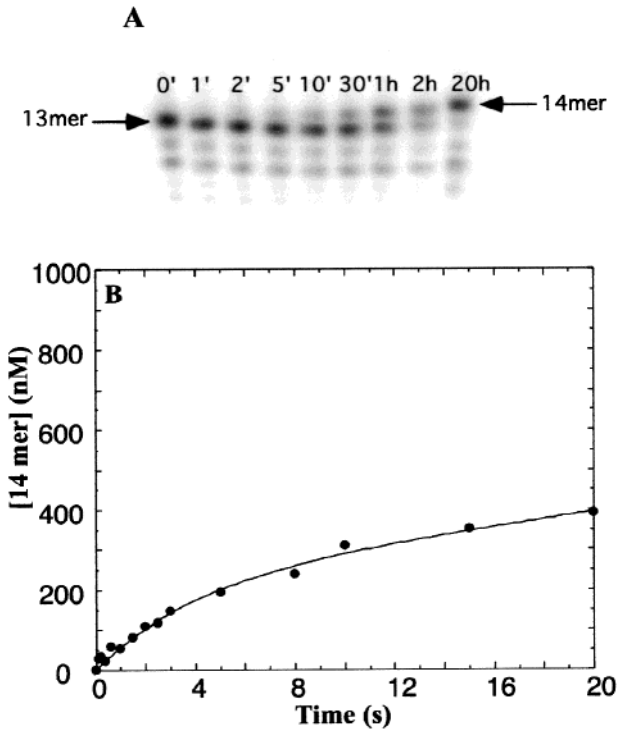

FIGURE 5: (A) dCDP incorporation by the parental RB69 gp43 (exo$^-$): a representative radioautograph to demonstrate dCDP incorporation by the parental enzyme, where equimolar amounts of PT and dCDP were used in the reaction. After incubation with the parental enzyme for 1 h, about 50% of the 13mer was converted into the 14mer. After 20 h, greater than 90% of the 13mer was converted into the 14mer, thus excluding the possibility that primer extension was caused by trace contamination of dCTP in the dCDP preparation. (B) Burst assay for dCDP incorporation by RB69 gp43. The 13/20mer (2 μM) was preincubated with RB69 gp43 (600 nM) and then mixed with an equal volume of 2 mM dCDP in a 20 mM Mg^{2+} containing Tris-HCl buffer to start the reaction, giving final concentrations of 13/20mer (1 μM), enzyme (300 nM), dCDP (1 mM), and 10 mM Mg^{2+}. The reactions were quenched at the indicated times and analyzed by gel electrophoresis. The solid line represents the best fit to the burst equation to give an amplitude, *A*, of 215 nM, a burst rate, k_{ob}, of 0.26 $\pm$ 0.07 s^{-1}, and a steady-state rate, k_{ss}, of 0.04 $\pm$ 0.01 s^{-1}.

reduction in the k_{pol} ratio (dCDP/dCTP), had the largest increase in K_d (82-fold) (Table 3).

DISCUSSION

Function of R482, K486, K560, and N564 in the Fingers Domain. The crystal structure of RB69 gp43 in a ternary complex depicts interactions between the four conserved residues in the fingers domain and the triphosphate moiety of incoming dNTP (Figure 1B) (*16*). As we have shown, when there are direct interactions between the conserved residue in the fingers and the triphosphate moiety, there is a larger effect on the kinetic parameters than if the interactions are indirect (i.e., mediated by water molecules). Our pre-steady-state data agree with the functional consequences inferred from the crystal structure in that the R482A and K560A mutants have severely impaired pol activity (Table 3). By contrast, the K486A and N564A mutants had only moderately diminished activity compared to the parental enzyme. The absence of a burst with the R482A and K560A mutants suggests that chemistry, or steps prior to the nucleotidyl transfer reaction, is rate-limiting. To explore this further, we determined the effect of substituting sulfur for the nonbridging oxygen in the α position. dNTPαS derivatives have been used with T4 and T7 DNA polymerases as well as with KF to determine whether chemistry was rate-limiting in the pol reaction. A small elemental effect, which was observed with each of these enzymes, was taken to mean that steps other than chemistry limited the rate of nucleotide addition (*5*, *34*, *35*). The difficulty in interpreting these results is that the magnitude of the elemental effect depends on the nature of the transition state for the pol reaction, which is not well enough understood with any of these polymerases to predict what the value should actually be if chemistry were indeed rate-limiting (*27*). Although we found small elemental effects with the parental RB69 gp43 as well as with the four finger domain mutants (Table 2), the observed ratios of k_{pol} (O/S) values determined with oxygen vs sulfur suggest that chemistry was not rate-limiting with either the parental or the mutant enzymes.

The kinetic parameters of the R482A and K486A mutants for dCTP incorporation differ from each other with respect to K_d and k_{pol} (Table 3) even though both basic residues interact with γ-phosphate oxygens. R482 makes a direct hydrogen bond to the γ-phosphate, whereas there is a hydrogen bond between K486 andthe γ-phosphate via a poorly ordered water molecule. Consequently, it would be predicted that the Ala for Lys replacement at residue 486 would have less of an effect on the activity than the Ala for Arg substitution at residue 482. This is what was found. The behavior of K560A reflects the importance of the H-bonds formed by the ϵ-amino group with both the α- and γ-phosphate oxygens on both K_d and k_{pol} (Figure 1B).

dNDPs Can Serve as Substrates for Primer Extension with the Parental Enzyme as Well as with Certain Mutants. After removing the contaminating exonucleases in the parental enzyme, we were able to detect dCDP incorporation by the parental enzyme as well as by several of the finger domain mutants (Table 3). The kinetic parameters for dCDP incorporation by the parental enzyme and finger domain mutants can be rationalized first as a disruption and then as a partial restoration with the mutants of the charge balance in the polymerase active site. In the parental enzyme, the triphosphate moiety of an incoming dNTP provides a layer of negative charge between the catalytic metal ions and the positively charged fingers residues R482, K486, and K560. With dCDP bound, this screening negative charge is partially removed, causing mutual repulsion between the positively charged fingers residues and the metal ions, thereby perturbing the substrate binding site and lowering the affinity for the incoming nucleoside diphosphate. The R482A mutant has an affinity for dCDP similar to that of the parental enzyme for dCTP (Table 3); the loss of the positive charge on R482 partially compensates for the loss of the negative charge on the nucleotide's γ-phosphate. It is still uncertain, however, if the k_{pol} of 0.5 s^{-1} for dCDP incorporation by the parental enzyme reflects the rate of conformational change or chemistry. Since we could not detect any dCDP incorporation by KF, this suggests that a different arrangement of basic residues in the fingers domain of RB69 gp43 vs KF may account for the variation in substrate utilization between the two enzymes.

Sequence of Binding Events for an Incoming dNTP: Comparison of RB69 DNA Polymerase with KF. Comparison of the apoenzyme and the ternary complex of RB69 gp43 is

informative with respect to conformational changes that take place during the reaction cycle. Since the four conserved fingers residues are far from the active site in the palm when the enzyme is in the apo or open form, they cannot engage the triphosphate of the incoming dNTP even after it is paired with its complementary template base unless the fingers domain rotates in toward the palm. Once the correctly bound dNTP is in place, the triphosphate tail could assist the fingers domain in completing the conformational change via charge−charge interactions. Were this to occur, it would result in binding of the dNTP as well as the PT terminus by the palm, the thumb and fingers excluding water from the active site. This process would also help to orient the OH group on the ribosyl moiety of the 3′-terminal nucleotide of the primer for in-line attack on the α-phosphorus atom of the bound dNTP (*16*).

On the basis of the structures of an E−dNTP binary complex and an E−DNA−dNTP ternary complex of Klentaq, Li et al. (*18*, *36*) suggested a different sequence for these events, namely, that the fingers domain (O helix in Klentaq) binds first to the triphosphate moiety of an incoming dNTP followed by a conformational change where the fingers rotate toward the palm delivering the incoming dNTP to the active site, thereby assembling a productive complex poised for chemistry. Our pre-steady-state kinetic results and inhibition studies with RB69 gp43 differ from those obtained with KF, suggesting a different sequence of events after substrate recognition by Klentaq or KF vs RB69 gp43. We would argue that the model suggested by Li et al. (*18*) does not apply to pol α family DNA polymerases, as represented by RB69 gp43, although it may be true for Klentaq, KF, and perhaps other nonreplicative DNA polymerases in the pol I family. We base this assertion on the following observations: (i) RB69 gp43, in contrast to KF or Klentaq, has a very weak affinity (K_d in the millimolar range) for incoming nucleotides with incorrect bases or sugars; (ii) RB69 gp43 has an even weaker affinity for PP_i (∼20 mM) than does KF (∼100 μM) (*30*); (iii) with RB69 gp43 only dNDPs with a matching base and a deoxyribosyl sugar are competitive inhibitors (K_i ∼ 500 μM) for NTPs complementary to the template base; (iv) other related compounds with triphosphate groups but with a missing or incorrect base or sugar fail to show significant inhibition of RB69 gp43 in standard primer extension assays.

It is possible that the movement of the fingers in RB69 gp43 (Figure 1A) (*16*) may be the rate-limiting step prior to chemistry and would be represented by the pre-steady-state k_{pol}. If correct, we believe that this conformational change occurs before the conserved residues in the fingers bind to the triphosphate tail of the incoming dNTP rather than their being delivered to the active site by the movement of the fingers as suggested by Li et al. (*18*). It is likely that incoming NTPs diffuse into the nucleoside binding pocket first; then only NTPs with both a complementary base and a deoxyribosyl sugar would have long enough residence times for subsequent interactions between the conserved residues in the fingers and the triphosphate tail prior to the chemical step. This is consistent with the lack of inhibition exhibited by noncomplementary dNTPs up to concentrations of 5 mM (*5*) and contrasts with the behavior of KF which discriminates less well against incorrect dNTPs at the binding step as shown by the following observations: (i) KF has similar K_d values for noncomplementary and complementary incoming dNTPs (Table 4) (*30*, *31*); (ii) noncomplementary dNTPs effectively inhibit correct dNTP incorporation; the K_i values for mismatched dNTPs are close to the K_d's for correct dNTPs (*33*); (iii) PP_i has a K_d value of 100 μM, close to that of incoming dNTPs (Table 4) (*32*). Thus, it appears that the initial binding of dNTPs to KF may involve only the interaction between the fingers domain and the triphosphate moiety, but not the base and sugar in the nascent nucleoside binding pocket of the enzyme.

The difference in behavior between RB69 gp43 and KF can be further rationalized by comparing the structure of the nucleotide binding sites of each enzyme in the open and closed forms (*14*, *16*, *18*, *37*). It can be seen that Y567, a highly conserved residue in RB69 gp43 important for fidelity (*38*) and an important feature of the nucleoside binding pocket, hardly moves when the enzyme goes from an open to a closed conformation (*16*). Superposition of the ternary complex and apoenzyme structures shows that the six carbon atoms in the phenyl ring of residue Y567 move an average of only 0.57 Å, although the α-carbon atom shifts by 1.39 Å. Another highly conserved residue, Y416, which serves as "sugar gate" for rNTP/dNTP discrimination (Yang et al., manuscript in preparation), occupies almost the same position in both the open and closed conformations. Y416 is equivalent to Y412 in Vent DNA pol (*39*) and Y254 in *ϕ*29 DNA pol (*40*), which are also in the pol α family. Single site mutants of these residues also have reduced discrimination between rNTPs and dNTPs (*39*, *40*). Superposition of the ternary complex and apoenzyme structures of RB69 gp43 shows that the ring atoms of Y416 move an average of only 0.78 Å, and the α-carbon atom shifts by 0.61 Å. Thus it would appear that the nucleoside binding pocket is already formed when RB69 gp43 is in the open conformation. This would favor binding of the correctly base-paired incoming dNTP, with its triphosphate tail and Mg^{2+} bound to the carboxylate ligands of the essential Asp residues in the enzyme.

The results with RB69 gp43, outlined above, differ from inferences about the order of dNTP binding based on structural studies with Klentaq (*18*) and from kinetic experiments performed with KF (*28*, *29*, *31*, *32*). As mentioned previously, the sequence of dNTP binding events envisioned by Li et al. (*18*) was based on crystal structures of the Klentaq−dNTP binary complex and on the Klentaq−PT−dNTP ternary complex. When the binding site for the incoming dNTP in the closed, ternary Klentaq−PT−dNTP complex is compared to the nascent nucleoside binding pocket in the open binary Klentaq−PT complex, large changes can be seen with respect to the relative positions of critical residues that comprise the nucleoside binding pocket: e.g., Y671 in Klentaq, equivalent to Y766 in KF, moves 4.80 Å as measured by the average movement of the aromatic ring in the open vs closed conformation (*18*). Another residue in Klentaq, F667, equivalent to F762 in KF, which is also part of the nucleoside binding pocket, moves 2.71 Å as measured by the average movement of the aromatic ring in the open and closed forms (*18*). These results indicate that residues which make up the nascent base pair binding pocket in Klentaq are not properly configured in the open conformation to permit nucleoside binding so it is not likely that the base and sugar of the incoming dNTP would bind

to the active site first, as we suggest happens with RB69 gp43. There is no problem, however, with the Klentaq binding to the triphosphate tail of the incoming dNTP first, followed by a conformational change to assemble a functional ternary complex as proposed by Li et al. (*18*).

It should be emphasized that our kinetic data cannot distinguish between (i) the fingers movement being triggered by binding of an incoming dNTP with its complementary base in the nucleoside binding pocket or (ii) locking in of the fingers (which probably flicker between open and closed conformations) into the closed form only in the presence of the complementary dNTP. Once the active site of the ternary complex is fixed in the optimal, geometrically configured closed form, then chemistry is extremely fast. There may be exceptions to this generally accepted scheme. For example, in the case of pol β, it has been suggested that the rate-limiting step is not the "open" to "closed" structural transition but instead is a conformation change triggered in the closed pol conformation by the correct incoming dNTP (*41*).

Is there any biological significance that can be attributed to these differences? We note first that RB69 gp43 and T4 gp43 are pol α family replicative DNA polymerases, while KF and Klentaq are pol I family repair polymerases. However, T7 DNA polymerase, a replicative polymerase, has been assigned to the pol I family on the basis of sequence similarities but behaves like RB69 gp43 with respect to discrimination at the dNTP binding step (very weak inhibition by noncomplementary dNTPs) (*42*). Another replicative polymerase, HIV RT, has a similar high degree of selectivity for ground-state nucleoside triphosphate binding as the DNA polymerases from phages RB69, T4, and T7. The K_d values for incorrect nucleoside triphosphates with HIV RT were 200−400-fold higher than for correct dNTPs (*43*). We also note that Y115, the functionally equivalent residue in HIV RT that corresponds to Y416 in RB69 gp43 and that makes up part of the sugar binding pocket, undergoes only a small displacement when going from the open to the closed form like RB69 gp43 (*44*, *45*). Despite this similarity between HIV RT and RB69 gp43 it has been stated that the initial interaction of the incoming nucleoside triphosphate with the two fingertip residues, K65 and R72, may induce closure of the fingers in HIV RT (*45*). Perhaps this issue deserves reexamination with HIV RT.

The importance of substrate discrimination during the initial binding step for a replicative enzyme has been discussed by Johnson (*24*), who pointed out that polymerization efficiency is diminished for DNA polymerases that fail to distinguish complementary from noncomplementary dNTPs during ground-state binding because dNTPs with mismatched bases are effective inhibitors of the primer extension reaction. It would seem then that it is the function of the DNA polymerase rather than the family to which it belongs that correlates best with the degree of dNTP selectivity. For DNA repair enzymes such as KF and Klentaq, reduced polymerization efficiency is less of an issue than it is for replicative DNA polymerases which have to extend primers rapidly with a high degree of precision and processivity.

ACKNOWLEDGMENT

We thank Dr. Catherine Joyce for critically reading the manuscript.

REFERENCES

1. Brautigam, C. A., and Steitz, T. A. (1998) *Curr. Opin. Struct. Biol. 8*, 54−63.
2. Steitz, T. A. (1993) *Curr. Opin. Struct. Biol. 3*, 31−38.
3. Braithwaite, D. K., and Ito, J. (1993) *Nucleic Acids Res. 21*, 787−802.
4. Wang, C. C., Yeh, L. S., and Karam, J. D. (1995) *J. Biol. Chem. 270*, 26558−26564.
5. Capson, T. L., Peliska, J. A., Kaboord, B. F., Frey, M. W., Lively, C., Dahlberg, M., and Benkovic, S. J. (1992) *Biochemistry 31*, 10984−10994.
6. Abdus Sattar, A. K., Lin, T. C., Jones, C., and Konigsberg, W. H. (1996) *Biochemistry 35*, 16621−11629.
7. Lin, T. C., Karam, G., and Konigsberg, W. H. (1994) *J. Biol. Chem. 269*, 19286−19294.
8. Lin, T. C., Wang, C. X., Joyce, C. M., and Konigsberg, W. H. (2001) *Biochemistry 40*, 8749−8755.
9. Wu, P., Nossal, N., and Benkovic, S. J. (1998) *Biochemistry 37*, 14748−14755.
10. Frey, M. W., Sowers, L. C., Millar, D. P., and Benkovic, S. J. (1995) *Biochemistry 34*, 9185−9192.
11. Beechem, J. M., Otto, M. R., Bloom, L. B., Eritja, R., Reha-Krantz, L. J., and Goodman, M. F. (1998) *Biochemistry 37*, 10144−10155.
12. Nossal, N. G. (1998) *Genetics 148*, 1535−1538.
13. Elisseeva, E., Mandal, S. S., and Reha-Krantz, L. J. (1999) *J. Biol. Chem. 274*, 25151−25158.
14. Wang, J., Sattar, A. K., Wang, C. C., Karam, J. D., Konigsberg, W. H., and Steitz, T. A. (1997) *Cell 89*, 1087−1099.
15. Shamoo, Y., and Steitz, T. A. (1999) *Cell 99*, 155−166.
16. Franklin, M. C., Wang, J., and Steitz, T. A. (2001) *Cell 105*, 657−667.
17. Delarue, M., Poch, O., Tordo, N., Moras, D., and Argos, P. (1990) *Protein Eng. 3*, 461−467.
18. Li, Y., Korolev, S., and Waksman, G. (1998) *EMBO J. 17*, 7514−7525.
19. Doublie, S., Tabor, S., Long, A. M., Richardson, C. C., and Ellenberger, T. (1998) *Nature 391*, 251−258.
20. Zhao, Y., Jeruzalmi, D., Moarefi, I., Leighton, L., Lasken, R., and Kuriyan, J. (1999) *Struct. Folding Des. 7*, 1189−1199.
21. Hopfner, K. P., Eichinger, A., Engh, R. A., Laue, F., Ankenbauer, W., Huber, R., and Angerer, B. (1999) *Proc. Natl. Acad. Sci. U.S.A. 96*, 3600−3605.
22. Rodriguez, A. C., Park, H. W., Mao, C., and Beese, L. S. (2000) *J. Mol. Biol. 299*, 447−462.
23. Hashimoto, H., Nishioka, M., Fujiwara, S., Takagi, M., Imanaka, T., Inoue, T., and Kai, Y. (2001) *J. Mol. Biol. 306*, 469−477.
24. Johnson, K. A. (1993) *Annu. Rev. Biochem. 62*, 685−713.
25. Doublie, S., and Ellenberger, T. (1998) *Curr. Opin. Struct. Biol. 8*, 704−712.
26. Yang, G., Lin, T., Karam, J., and Konigsberg, W. H. (1999) *Biochemistry 38*, 8094−8101.
27. Herschlag, D., Piccirilli, J. A., and Cech, T. R. (1991) *Biochemistry 30*, 4844−4854.
28. Astatke, M., Grindley, N. D., and Joyce, C. M. (1998) *J. Mol. Biol. 278*, 147−165.
29. Astatke, M., Ng, K., Grindley, N. D., and Joyce, C. M. (1998) *Proc. Natl. Acad. Sci. U.S.A. 95*, 3402−3407.
30. Kuchta, R. D., Benkovic, P., and Benkovic, S. J. (1988) *Biochemistry 27*, 6716−6725.
31. Carroll, S. S., Cowart, M., and Benkovic, S. J. (1991) *Biochemistry 30*, 804−813.
32. Kuchta, R. D., Mizrahi, V., Benkovic, P. A., Johnson, K. A., and Benkovic, S. J. (1987) *Biochemistry 26*, 8410−8417.
33. Eger, B. T., Kuchta, R. D., Carroll, S. S., Benkovic, P. A., Dahlberg, M. E., Joyce, C. M., and Benkovic, S. J. (1991) *Biochemistry 30*, 1441−1448.
34. Patel, S. S., Wong, I., and Johnson, K. A. (1991) *Biochemistry 30*, 511−525.
35. Mizrahi, V., Henrie, R. N., Marlier, J. F., Johnson, K. A., and Benkovic, S. J. (1985) *Biochemistry 24*, 4010−4018.

36. Li, Y., Kong, Y., Korolev, S., and Waksman, G. (1998) *Protein Sci. 7*, 1116−1123.
37. Beese, L. S., Derbyshire, V., and Steitz, T. A. (1993) *Science 260*, 352−355.
38. Bebenek, A., Dressman, H. K., Carver, G. T., Ng, S., Petrov, V., Yang, G., Konigsberg, W. H., Karam, J. D., and Drake, J. W. (2001) *J. Biol. Chem. 276*, 10387−10397.
39. Gardner, A. F., and Jack, W. E. (1999) *Nucleic Acids Res. 27*, 2545−2553.
40. Bonnin, A., Lazaro, J. M., Blanco, L., and Salas, M. (1999) *J. Mol. Biol. 290*, 241−251.
41. Vande Berg, B. J., Beard, W. A., and Wilson, S. H. (2001) *J. Biol. Chem. 276*, 3408−3416.
42. Wong, I., Patel, S. S., and Johnson, K. A. (1991) *Biochemistry 30*, 526−537.
43. Kati, W. M., Johnson, K. A., Jerva, L. F., and Anderson, K. S. (1992) *J. Biol. Chem. 267*, 25988−25997.
44. Jacobo-Molina, A., Ding, J., Nanni, R. G., Clark, A. D., Jr., Lu, X., Tantillo, C., Williams, R. L., Kamer, G., Ferris, A. L., Clark, P., et al. (1993) *Proc. Natl. Acad. Sci. U.S.A. 90*, 6320−6324.
45. Huang, H., Chopra, R., Verdine, G. L., and Harrison, S. C. (1998) *Science 282*, 1669−1675.

BI0119924